



A CYCLOSTATIONARY APPROACH IN EXTRACTING MODULATION FEATURE FROM FAN VIBRATIONS

Ning CHU, Shiyang LI, Dazhuan WU

Zhejiang University, Zheda road No.38, 310027 Hangzhou, China

SUMMARY

Vibration signals related to fan aerodynamic performance are generally transient, non-stationary and non-linear. To extract aerodynamic-related features from these complicated signals, this paper presents an improved cyclostationary approach and employs an enhanced envelop spectrum to detect the modulating, harmonic and coupled frequencies, as well as to reconstruct principle modulating intensities. These modulation-related components have strong links with the flow-induced excitation, and can provide an alternative way to reveal the fan aerodynamics. Finally proposed approach is validated by typical simulation and axial-flow fan experiments.

INTRODUCTION

Since decades, the direct relation between the flow-induced excitation source and fan vibration-noise has been a hot topic, but not yet elaborated clearly. It is considered that the flow-induced effect not only reinforces the characteristic components at the shaft frequency (SF) and blade passing frequency (BPF), but also excites the non-linear components at harmonic (HF) and coupled frequencies (CF). Therefore, such flow-induced effect could be regarded as main excitation source that aggravates the fan vibration and noise. However, it is not easy for conventional signal processing methods such as power-spectrum based and time-frequency based analysis to detect characteristic components and reconstruct spectral intensities. This is because vibration and acoustic signals involve in hidden modulation mechanism. In fact, due to the quasi-periodic and rapid rotations of fan shaft and blades, the flow-induced effect inherently generates a transient and broadband carrier signal, meanwhile, this irregularly changing carrier is modulated mainly by the SF and BPF components. In other words, the flow-induced effect can not only reinforces the modulation-related components, but also excites by-product harmonic and coupled frequencies. Indeed, the vibration and acoustic signal in fan operation turns out to be modulated, non-stationary and non-linear. In order to reveal the flow-induced effects and aerodynamic performance, it is highly necessary to demodulate such a complicated signal and extract its modulation-related components.

These days, the cyclostationary analysis has been a powerful tool for the vibration based condition monitoring. Cyclostationarity has been systematically developed by Gardner *et al.* and widely used in communication system and mechanical signal analysis [3-4]. Since then, many researchers [5-10] have developed advanced cyclostationary analysis in condition monitoring and fault detection of rotating machines. It has been successfully applied in fault diagnosis of rolling shaft, roller bearing and gear box [1-2]. In particular, Antoni *et al.* [11-14] established the cyclostationarity model and proposed a general methodology for analyzing complicated cyclostationary signals, especially introducing the cyclical spectral coherence to successfully detect the character frequencies in the vibration signals of the shafts and blades, gear boxes, as well as propellers and pumps. Botero *et al.* [15] adopted the cyclostationarity to detect the rotating stall instability and the number of stall cells in turbines. Napolitano [16] reviewed the application, new trends and limitations of cyclostationarity, which provided a comprehensive understanding of cyclostationarity to better serve the turbine design and fault diagnosis. The advantages of cyclostationary analysis are that it can comprehensively reveal the weak and hidden periodic features from the complicated waveforms of turbine signals, and can also extract the modulation-related components which are excited by a quasi-periodic excitation sources. However, most of the classical methods take the vibrational signal as a wide-sense stationary process or distinctly periodic one, thus they are incompetent to deal with signal cyclostationarity, and they neglect the hidden-period statistical moments.

To the best of authors' knowledge, few articles have revealed the quantitative relationship between flow-induced excitation and modulation-related components related to fan aerodynamic performance. This paper aims to improve the cyclostationary method and employ enhance envelop spectrum to characterize transient, non-stationary and broadband signals. The rest of paper is organized as: Section I briefly introduces the cyclostationarity of rotational machine. A modulation model of vibrational signals is established in Section II. An enhanced envelop spectrum is employed to quantitatively analyze modulation model in Section III. Through typical simulations and axial fan experiments in Section IV and V. Finally Section VI concludes this paper.

CYCLOSTATIONARY ANALYSIS METHODS

The cyclostationarity is the second-order statistical moment and can indicate a periodically time-varying autocorrelation function, defined as in Eq.(1).

$$R_x(t, \tau) = \lim_{N \rightarrow \infty} \frac{1}{2N+1} \sum_{n=-N}^N x(t+nT_0 + \frac{\tau}{2})x^*(t+nT_0 - \frac{\tau}{2}) = R_x(t+T_0, \tau) \quad (1)$$

where T_0 and τ denote the period and the time lag, respectively ($\tau \leq T_0$). The cyclic autocorrelation function is defined as the extracted coefficients by expanding the autocorrelation function into a Fourier series, as shown in Eq. (2).

$$R_x^\alpha(\tau) = \lim_{T \rightarrow \infty} \frac{1}{T} \int_T x(t + \frac{\tau}{2})x^*(t - \frac{\tau}{2})e^{-j2\pi\alpha t} dt \quad (2)$$

where α is known as the cyclic frequency of the signal and its inverse as the cycle; j is the imaginary unit. The spectral correlation density (SCD) function is obtained by performing a Fourier transform of the cyclic autocorrelation function:

$$SC_x^\alpha(f) = \int_{-\infty}^{\infty} R_x^\alpha(\tau)e^{-j2\pi f\tau} d\tau. \quad (3)$$

For better understanding of its physical meanings, another definition developed by Antoni [7] is briefly introduced as follows. It should be claimed that these two definitions are essentially

identical. Firstly, Eq. (4) is introduced as a pure second-order cyclostationary signal with a random stationary carrier $v(t)$:

$$x(t) = \cos(2\pi\alpha_0 t) \cdot v(t) \quad (4)$$

To detect its hidden periodicity $T_0 = 1/\alpha_0$, a spectral correlation that measures the interaction between two spectral components at frequencies f_1 and f_2 is introduced as

$$\text{corr}_x(f_1, f_2) = \lim_{\Delta f \rightarrow 0} \frac{1}{\Delta f} \lim_{T \rightarrow \infty} \frac{1}{T} \int_T x_{\Delta f}(t; f_1) x_{\Delta f}^*(t; f_2) e^{-j2\pi(f_1 - f_2)t} dt \quad (5)$$

where $x_{\Delta f}(t; f)$ is the filtered version of signal $x(t)$ through a frequency band of width Δf centered at frequency f , and the order of two limits cannot be interchanged. By changing the variables $f = (f_1 + f_2) / 2$, $\alpha = f_1 - f_2$, Eq. (5) turns to the second definition of the SCD as:

$$SC_x^\alpha(f) = \lim_{\Delta f \rightarrow 0} \frac{1}{\Delta f} \lim_{T \rightarrow \infty} \frac{1}{T} \int_T x_{\Delta f}(t; f + \frac{\alpha}{2}) x_{\Delta f}^*(t; f - \frac{\alpha}{2}) e^{-j2\pi\alpha t} dt \quad (6)$$

Eq. (6) is more intuitive and it represents a density of correlation of two spectral components spaced apart by α . However, some small vibration signatures will be masked in the spectral correlation density due to the spectral scaling effect. And more often, the degree of the cyclostationarity, which is a relative measure for the spectral correlation, is more concerned in detecting the vibration signature. Hence, the cyclical spectral coherence is defined as follows [13,14]:

$$\gamma_x^\alpha(f) = \frac{\text{corr}_x(f + \frac{\alpha}{2}, f - \frac{\alpha}{2})}{\sqrt{P_x(f + \frac{\alpha}{2})P_x(f - \frac{\alpha}{2})}} = \frac{SC_x^\alpha(f)}{\sqrt{SC_x^0(f + \frac{\alpha}{2})SC_x^0(f - \frac{\alpha}{2})}} \quad (7)$$

where $P_x(f)$ is the power spectral density and $SC_x^0(f) \equiv P_x(f)$. Thus enhanced envelop spectrum is:

$$\gamma_x(\alpha) = \int_{-\infty}^{\infty} SC_x^\alpha(f) df \quad (8)$$

It is noted that $\gamma_x(\alpha)$ in Eq.(8) can transform an image of power spectral density into a concise curve of enhanced envelop spectrum. Considering the impulsive response of sensor measurements $y(t) = h(t) \otimes x(t)$, the spectral correlation density and spectral coherence can be extended as:

$$SC_y^\alpha(f) = H(f + \frac{\alpha}{2}) H^*(f - \frac{\alpha}{2}) SC_x^\alpha(f) \quad (9)$$

$$\gamma_y^\alpha(f) = \frac{H(f + \frac{\alpha}{2}) H^*(f - \frac{\alpha}{2})}{\left| H(f + \frac{\alpha}{2}) \right| \left| H(f - \frac{\alpha}{2}) \right|} \gamma_x^\alpha(f)$$

where $h(t)$ represents the impulse response, and transfer function $H(f)$ is the spectrum of $h(t)$.

SIGNAL MODEL OF FAN VIBRATION

The vibration model for fan operation can be derived according to rolling-element bearings with inner-race faults, which is widely used to provide an intuitive understanding to bearing fault signals [3,7,10,12]. A simplified version without the random slips is provided as following:

$$y(t) = h(t) \otimes \left\{ \sum_{n=1}^N \delta(t - nT) [1 + q(t)] \right\} + n(t) \quad (10)$$

where $h(t)$ denotes the impulse response of sensor to a single impact, and T is the inter-arrival time between two consecutive impacts. $q(t) = q(t+P)$ is the periodic modulation with period P due to the load distribution, given that the inner-race defect will move in and out of the bearing load zone. The vibration will be strongest when the defect is in the load zone, and weakest when it is out of the load zone. Therefore, the period P is related to the shaft rotating frequency for a simple rolling-element bearing. $n(t)$ accounts for an additive background noise including other vibration sources. When fan is running, the steady and unsteady fluid forces on the fan blades are imposed on the bearing. The steady fluid force could impart much larger load than the original steady load, and the unsteady fluid force can generate oscillatory bearing load at BPF. Hence, even without any incipient fault in the bearing, the vibration signals can still be modulated by the steady and unsteady load as:

$$y(t) = h(t) \otimes \{v(t)[1+q_f(t)]\} + n(t) \quad (11)$$

where $v(t)$ is the carrier from random vibrations, and $q_f(t)$ denotes the amplitude modulation due to the unsteady bearing load. For simplicity, impulse response $h(t)$ is omitted temporally. But it can be considered with Eq. (9).

ENHANCED ENVELOP SPECTRUM FOR DEMODULATION

Based on vibration signal model in Eq. (11), an amplitude modulation (AM) signal with infinite modulation components is embodied as:

$$x(t) = [1 + \sum_{i=1}^N A_i \cos(2\pi\alpha_i t)] \cdot v(t) \quad (12)$$

where A_i is the amplitude of the modulating signal and α_i is the modulating frequencies with $\alpha_{i+1} > \alpha_i \geq 0$. Then the AM signal is filtered by a narrow frequency band $[f-\Delta f/2, f+\Delta f/2]$ as:

$$x_{\Delta f}(t; f_1) = v_{\Delta f}(t; f_1) + \sum_{i=1}^N \frac{A_i}{2} [v_{\Delta f}(t; f_1 - \alpha_i) + v_{\Delta f}(t; f_1 + \alpha_i)] \quad (13)$$

$$x_{\Delta f}(t; f_2) = v_{\Delta f}(t; f_2) + \sum_{k=1}^N \frac{A_k}{2} [v_{\Delta f}(t; f_2 - \alpha_k) + v_{\Delta f}(t; f_2 + \alpha_k)] \quad (14)$$

Then inserting Eq. (12-14) into Eq. (5):

$$\begin{aligned} corr_x(f_1, f_2) = & corr_v(f_1, f_2) + \sum_{i=1}^N \frac{A_i}{2} [corr_v(f_1 - \alpha_i, f_2) + corr_v(f_1 + \alpha_i, f_2)] \\ & + \sum_{k=1}^N \frac{A_k}{2} [corr_v(f_1, f_2 - \alpha_k) + corr_v(f_1, f_2 + \alpha_k)] \\ & + \sum_{i=1}^N \sum_{k=1}^N \frac{A_i A_k}{4} [corr_v(f_1 - \alpha_i, f_2 - \alpha_k) \\ & + corr_v(f_1 - \alpha_i, f_2 + \alpha_k) + corr_v(f_1 + \alpha_i, f_2 - \alpha_k) + corr_v(f_1 + \alpha_i, f_2 + \alpha_k)] \end{aligned} \quad (15)$$

Where $corr_v(f_1, f_2) = P_v(f)$ is the power spectral density of carrier $v(t)$. As $v(t)$ being random vibration, any spectral correlation in $v(t)$ turns to be zero when two involved frequencies are not

identical. By changing the variables $a = f_1 - f_2$, and $f = (f_1 + f_2)/2$, Eq. (15) are categorized into four components as shown in Eq.(16):

$$corr_x(f_1, f_2) = SC_x^\alpha(f) = \begin{cases} (1 + \sum_i^N \frac{A_i^2}{2}) P_v(f), & \text{if } a = 0 & \text{(I)} \\ A_i P_v(f), & \text{if } a = a_i & \text{(II)} \\ \frac{A_i^2}{4} P_v(f), & \text{if } a = 2a_i & \text{(III)} \\ \frac{A_i A_k}{2} P_v(f), & \text{if } \alpha = |\alpha_i \pm \alpha_k|, i > k & \text{(IV)} \end{cases} \quad (16)$$

(I) power spectral density $P_v(f)$ of carrier $v(t)$, which is amplitude-modulated by $(1 + \sum_i^N \frac{A_i^2}{2})$,

(II) modulated intensity $A_i P_v(f)$ at modulation frequency a_i , including SF and BPF.

(III) harmonic intensity $\frac{A_i^2}{4} P_v(f)$ at the twice harmonic frequency $2a_i$,

(IV) coupled components $\frac{A_i A_k}{2} P_v(f)$ at coupled frequency $|a_i \pm a_k|, i > k$.

The corresponding spectral coherence $\gamma_x^\alpha(f)$ are shown in the Eq. (17):

$$\gamma_x^\alpha(f) = \begin{cases} 1, & \text{if } a = 0 & \text{(I)} \\ A_i / (1 + \sum_i^N \frac{A_i^2}{2}), & \text{if } a = a_i & \text{(II)} \\ \frac{A_i^2}{4} / (1 + \sum_i^N \frac{A_i^2}{2}), & \text{if } a = 2a_i & \text{(III)} \\ \frac{A_i A_k}{2} / (1 + \sum_i^N \frac{A_i^2}{2}), & \text{if } \alpha = |\alpha_i \pm \alpha_k|, i > k & \text{(IV)} \end{cases} \quad (17)$$

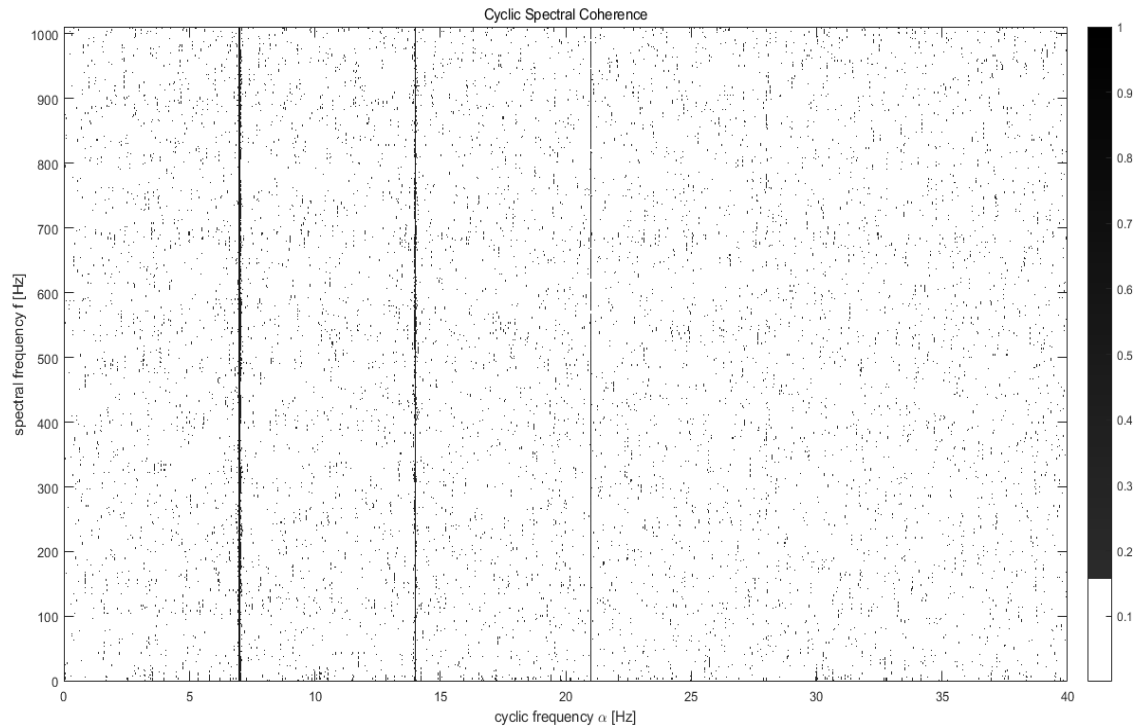
It is worth noting that the spectral coherence $\gamma_x^\alpha(f)$ is better to use than spectral correlation density $SC_x^\alpha(f)$, since $\gamma_x^\alpha(f)$ can reveal the degree of modulation intensity and avoid the influence of random carrier vibrations.

SIMULATIONS ON CYCLOSTATIONARITY RECONSTRUCTION

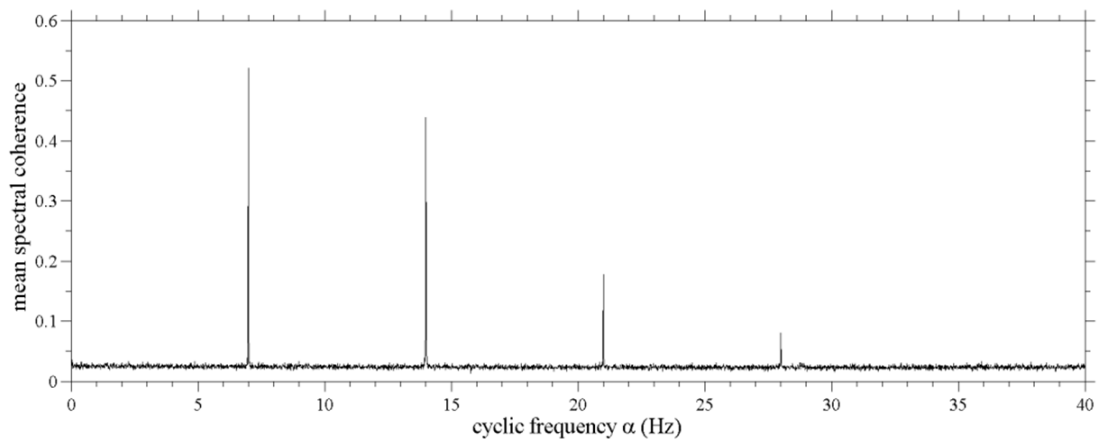
Before cyclostationarity analysis, two synthetic signals are adopted to verify the derived spectral coherence $\gamma_x^\alpha(f)$ in Eq.(17). For simplicity, synthetic signals contain only two modulation components as:

$$x(t) = [1 + \cos(2\pi\alpha_1 t) + \cos(2\pi\alpha_2 t)] \cdot v(t) . \quad (18)$$

For the first synthetic signal, the modulating frequencies are set as $\alpha_1 = 7 \text{ Hz}$, $\alpha_2 = 14 \text{ Hz}$, where one is another's harmonic. This case exists widely in rotating machinery vibrations. For the second, the modulating frequencies are set as $\alpha_1 = 10 \text{ Hz}$, $\alpha_2 = 14 \text{ Hz}$, where two modulating components are independent and irrelevant modulating components. Here a white Gaussian noise is used for random carrier signal $v(t)$. The sampling frequency is set to 1000 Hz.

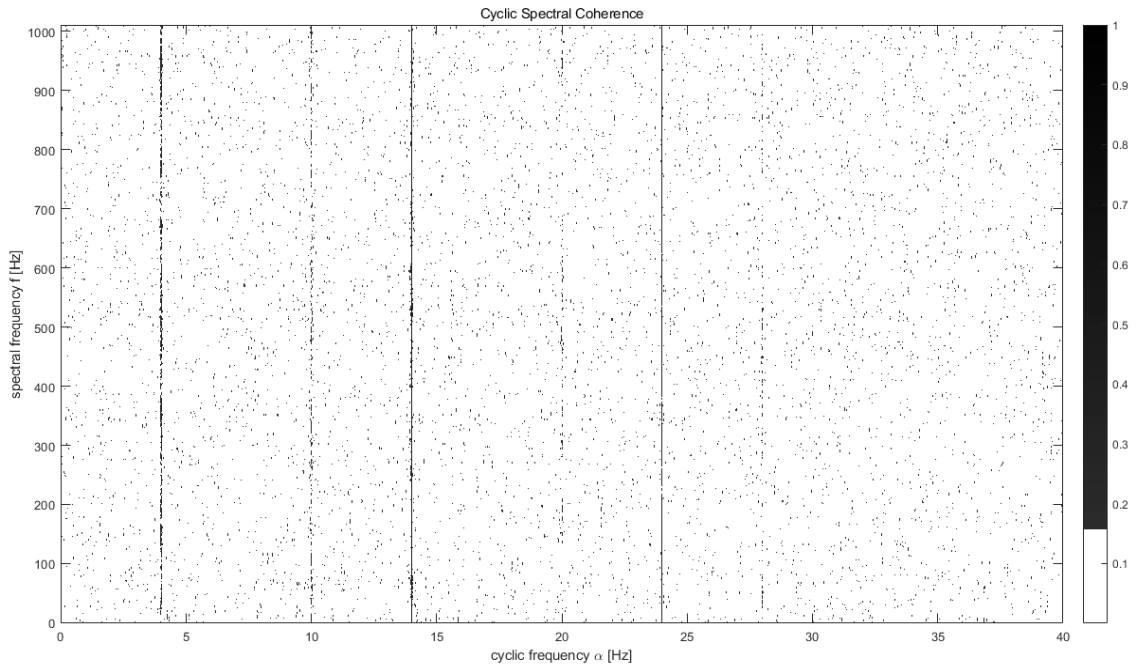


(a)

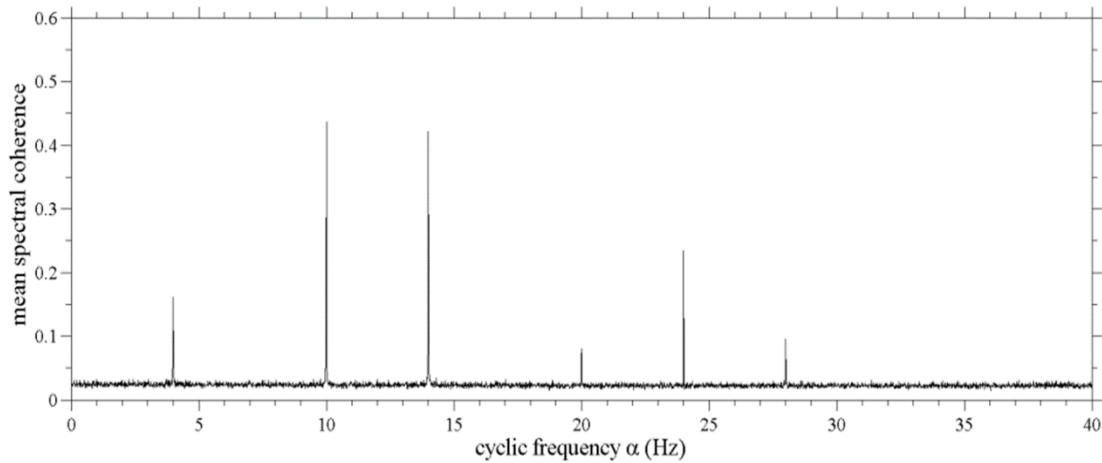


(b)

Figure 1: (a) spectral coherence $\gamma_x^\alpha(f)$ (b) enhanced envelop spectrum $\gamma_x(\alpha)$ with $\alpha_1 = 7$, $\alpha_2 = 14 \text{ Hz}$



(a)



(b)

Figure 2: (a) spectral coherence $\gamma_x^\alpha(f)$ (b) enhanced spectral coherence $\gamma_x(\alpha)$ with $\alpha_1 = 10, \alpha_2 = 14$ Hz

In fact, the signal $x(t)$ in Eq.(18) is a non-stationary signal, since its probability density function (PDF) is time-dependent and its statistical moments are time-varying. Therefore, this non-stationarity constrains the use of the state-of-the-art methods like STFT, WT and EMD etc. Owing to the periodical working mode of rotating machine, the PDF of $x(t)$ varies periodically with time, since $x(t)$ inherently has the periodic characteristics due to the modulation components. Compared with the conventional methods, cyclostationary analysis can extract the modulation components. For the first case, harmonic and coupled frequencies will mix up. Therefore, only four cyclic frequencies with non-zero values exist in the image of power spectral coherence. As displayed in Fig. 1(a), the spectral lines can be distinguished in the gray-level images. For the second, the harmonics and coupled components will not mix up, thus six spectral lines are detected clearly in Fig. 2(a). In addition, Fig. 1(b) and Fig. 2(b) display the enhanced envelop spectrum $\gamma_x(\alpha)$ in Eq.(8) alone frequency axis. Moreover, Table 1 demonstrates the performances of detecting

modulated frequencies and reconstructing modulated intensities for other cases of amplitude modulations.

Table 1: Detection of modulated frequency and reconstruction of modulated intensity

	Cyclic frequency α_i (Hz)			Intensity A_i (Unit)			
Simulation	30	50	65	1	1	1	1
Estimation	30	50	65	1.00	1.00	1.00	1.14
Error (%)	0	0	0	0	0	0	14.29%
Simulation	30	50	65	1	1	2	3
Estimation	30	50	65	1.00	1.27	2.25	2.75
Error (%)	0	0	0	0	26.92%	12.5%	12.5%
Simulation	30	40	60	1	1	1	1
Estimation	30	40	60	1.00	1.02	0.94	0.87
Error (%)	0	0	0	0	2.56%	5.84%	12.82%

FAN DATA TESTS ON CYCLOSTATIONARITY DETECTION

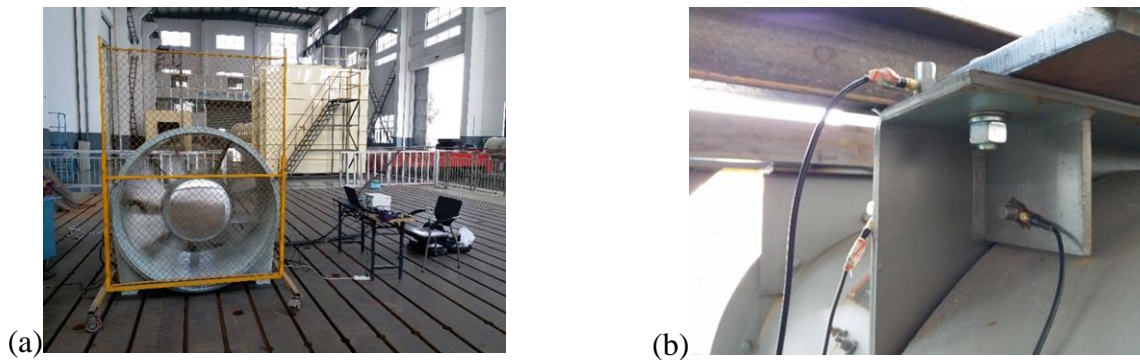
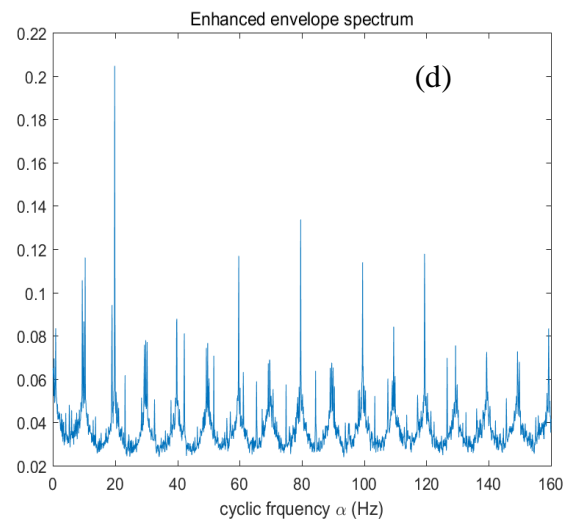
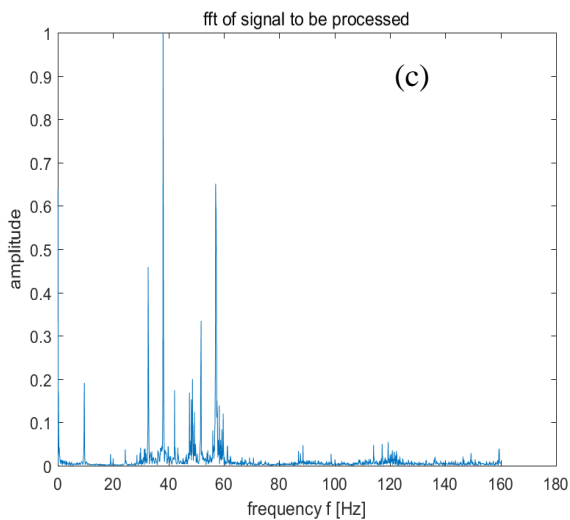
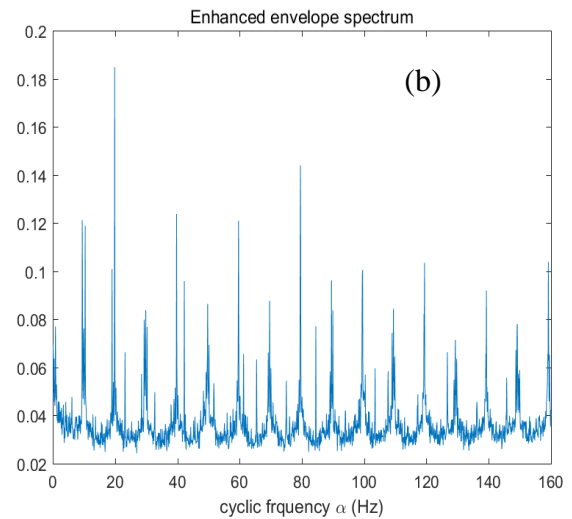
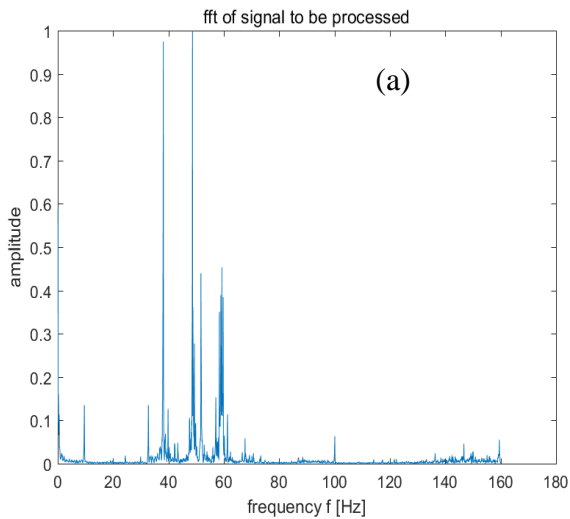


Figure 3: An axial-flow fan in experiments (a) and three sets of accelerometers (b).

Table 2. Parameters of tested axial fan.

Fan type	Subway fan
Fan parameters	
model	DTF Axial Fan
Air volume	$118800m^3/h$
Full pressure	$250Pa$
Rotating speed	985r/min
power	37kW
Power supply	Three-phase AC/380V/50HZ
Operating temperature	250°C below
weight	1559kg

The vibration signals are collected from an axial-flow fan as shown in Fig.3(a), which serves the ventilation in metro system. The rated parameters of this fan are of 75 km³/h output, 37 kW, shaft rotating frequency 1450 rpm (24.17 Hz), and BPF 193.33 Hz (8 blades). Three accelerometers are used as ECON SN J1165, ECON SN 05127 and PCB SN LW 186548 in Fig.3(b).



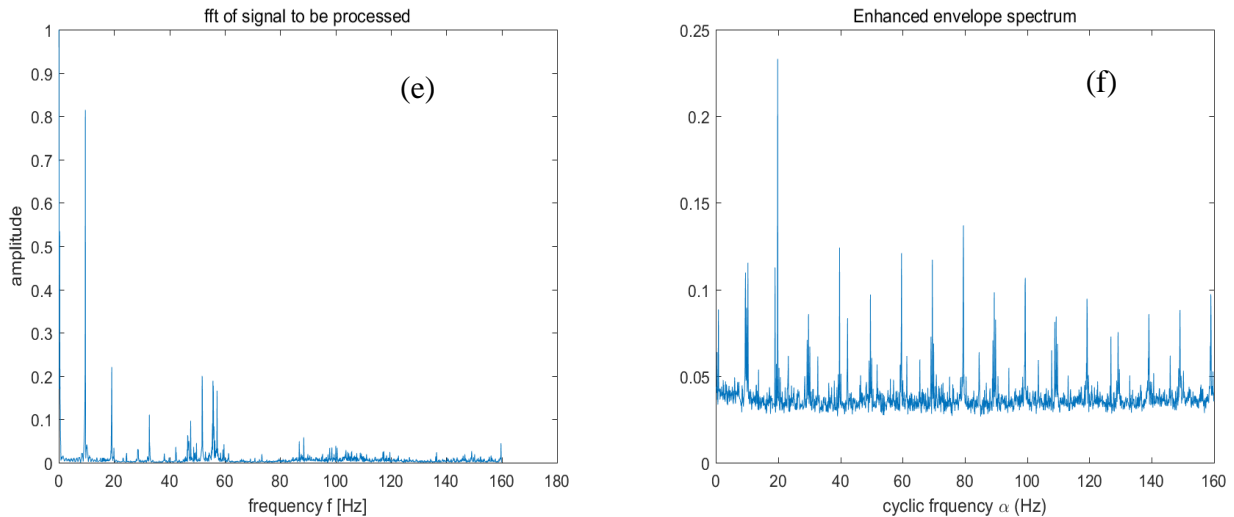


Figure 4: Foundation loosening:
(a)(c)(e) *fft-based spectrum*, (b)(d)(f) *enhanced envelop spectrum $\gamma_x(\alpha)$*

When the axial-flow fan is running at 10 Hz, the vibrational signals are sampled simultaneously by three accelerometers according to experimental setup in Fig.3. The power spectrum of signals at one sensor is shown in Fig. 4(a). It is easy to see a peak at 10 Hz, and this result indicates few of harmonic and coupled components. Unfortunately, conventional PSD method fails to detect the BPF at 80 Hz. On the contrary, in Fig. 4(b), the enhanced envelop spectrum $\gamma_x(\alpha)$ cannot only show the 10 Hz peak, but also reveal its multiple harmonics, especially the BPF at 80 Hz as a local peak. In the case of loosening one of the four bolts at fan foundation in Fig.4(c), the PSD changes as the peak at 50 Hz disappears. As for the enhanced envelop spectrum $\gamma_x(\alpha)$ in Fig.4(d), it can still obtain the most of key features of rotating frequencies. Moreover, the correlation coefficient between Fig.4(b) and Fig.4(d) is nearly 0.82, which can indicate some defect such as the foundation loosening. When the four bolts are totally relaxed in Fig.4(e-f), the PSD severely deteriorates and only gives the 10 Hz peak and some of harmonics, but the average spectral coherence can be able to tell the shaft rotation at 10 Hz, complete harmonics (2X in particular), as well as the BPF at 80 Hz. Moreover, the correlation coefficient between Fig.4(b) and Fig.4(f) is below nearly 0.67, which can be used as the fault diagnosis for severe bolts loosening.

CONCLUSION AND PERSPECTIVE

To extract the key features of vibration signals related to fan aerodynamics, this paper improves the cyclostationarity method by employing an enhanced envelop spectrum to deal with the transient, non-stationary and broadband signals. Through typical simulations and axial fan experiments, the enhanced envelop spectrum can provide a quantitative way to recognize the feature frequency components (SF, BPF, HF, CF etc.) of axial-flow fan during the normal and abnormal conditions. However, in order to suppress the mechanical interference and background impulse noise, it is promising to combine Kurtosis spectrum [22] and cyclostationarity. Comparing to vibrational signals, acoustic sources will be more convenient to analyze the fan aerodynamic and aeroacoustic performance. Therefore, it is more interesting but challenging to localize the acoustic sources by adequate array of microphone sensors in remote and non-contact measurements [18].

ACKNOWLEDGEMENT

This work is supported by the Natural Science Foundation of China (NSFC) 61701440, the National Program on Key Research Project of China 2016YFF0203300, and the Fundamental Research Funds for the Central Universities of China 2017QNA4015. Authors appreciate the valuable

discussions with Prof. Jérôme Antoni from INSA-Lyon (France). Many thanks to Dr. Song Yongxing, Dr. Wu Kelin in author's lab for experiment design and lay-out.

BIBLIOGRAPHY

- [1] R. B. Randall, J. Antoni, S. Chobsaard – *The relationship between spectral correlation and envelope analysis in the diagnostics of bearing faults and other cyclostationary machine signals*. Mechanical Systems & Signal Processing, 15(5), 945-962, **2001**
- [2] C. Capdessus, M. Sidahmed, J. L. Lacoume – *Cyclostationary processes: application in gear fault early diagnosis*. Mechanical Systems & Signal Processing, 14(3):371-385, **2000**.
- [3] I. Antoniadis, G. Glossiotis – *Cyclostation analysis of rolling element bearing vibration signals*. Journal of Sound & Vibration, 248(5):829-845, **2001**.
- [4] W. A. Gardner – *Introduction to Random Processes: with applications to signals and systems*. Macmillan Publishing Company, **1986**
- [5] W. Gardner – *Measurement of spectral correlation*. IEEE Transactions on Acoustics, Speech, and Signal Processing, 34(5), 1111-1123, **1986**.
- [6] L. Bouillaut, M. Sidahmed – *Cyclostationary and Bilinear Approaches for Gears Vibrating Signals*. Key Engineering Materials, 167-168:354-362, **1999**.
- [7] I. Antoniadis, G. Glossiotis – *Cyclostationary analysis of rolling-element bearing vibration signals*. Journal of sound and vibration, 248(5), 829-845, **2001**.
- [8] G. Dalpiaz, A. Rivola, R. Rubini – *Effectiveness and sensitivity of vibration processing techniques for local fault detection in gears*. Mechanical systems and signal processing, 14(3), 387-412, **2000**.
- [9] Z. K. Zhu, Z. H. Feng, F. R. Kong – *Cyclostationarity analysis for gearbox condition monitoring: Approaches and effectiveness*. Mechanical Systems & Signal Processing, 19(3):467-482, **2005**.
- [10] R. Boustany, J. Antoni – *A subspace method for the blind extraction of a cyclostationary source: Application to rolling element bearing diagnostics*. Mechanical Systems and Signal Processing, 19(6), 1245-1259, **2005**.
- [11] J. Antoni, J. Daniere, F. Guillet – *Effective vibration and analysis of IC engines using cyclostationarity Part I—A methodology for condition monitoring*. Journal of Sound & Vibration, 257(5):815-837, **2002**.
- [12] J. Antoni – *Cyclic spectral analysis of rolling-element bearing signals: facts and fictions*. Journal of Sound and vibration, 304(3), 497-529, **2007**.
- [13] J. Antoni – *Cyclic spectral analysis in practice*. Mechanical Systems & Signal Processing, 21(2):597-630, **2007**.
- [14] J. Antoni – *Cyclostationarity by examples*. Mechanical Systems & Signal Processing, 23(4):987-1036, **2009**.
- [15] F. Botero, V. Hasmatuchi, S. Roth, M. Farhat – *Non-intrusive detection of rotating stall in pump-turbines*. Mechanical Systems and Signal Processing, 48(1), 162-173, **2014**.
- [16] A. Napolitano – *Cyclostationarity: Limits and generalizations*. Signal Processing, 120, 323-347, **2016**.
- [17] S. Delvecchio, G. D'Elia, G. Dalpiaz – *On the use of cyclostationary indicators in IC engine quality control by cold tests*. Mechanical Systems & Signal Processing, 60-61:208-228, **2015**.

- [18] C. Cheong, P. Joseph – *Cyclostationary spectral analysis for the measurement and prediction of wind turbine swishing noise*. Journal of sound and vibration, 333(14), 3153-3176, **2014**.
- [19] Q. Leclere, L. Pruvost, E. Parizet – *Angular and temporal determinism of rotating machine signals: The diesel engine case*. Mechanical Systems and Signal Processing, 24(7), 2012-2020, **2010**.
- [20] M. Poirier, M. Gagnon, A. Tahan, A. Coutu, J. Chamberland-lauzon – *Extrapolation of dynamic load behaviour on hydroelectric turbine blades with cyclostationary modelling*. Mechanical Systems and Signal Processing, 82, 193-205, **2017**.
- [21] J. Antoni, D. Hanson – *Detection of surface ships from interception of cyclostationary signature with the cyclic modulation coherence*. IEEE Journal of Oceanic Engineering, 37(3), 478-493, **2012**.
- [22] J. Antoni, G. Xin, N. Hamzaoui, – *Fast Computation of the Spectral Correlation*, Mechanical Systems and Signal Processing, Elsevier, **2017**.